arXiv:0710.5104v1 [quant-ph] 26 Oct 2007

Casimir forces between arbitrary compact objects: Scalar and electromagnetic field

T. Emig[1,2] **and R. L. Jaffe**[3]

[1] Institut für Theoretische Physik, Universität zu Köln, Zülpicher Strasse 77, 50937 Köln, Germany

[2] Laboratoire de Physique Théorique et Modèles Statistiques, CNRS UMR 8626, Bât. 100, Université Paris-Sud, 91405 Orsay cedex, France

[3] Center for Theoretical Physics, Laboratory for Nuclear Science, and Department of Physics, Massachusetts Institute of Technology, Cambridge, MA 02139, USA

Abstract. We develop an exact method for computing the Casimir energy between arbitrary compact objects, both with boundary conditions for a scalar field and dielectrics or perfect conductors for the electromagnetic field. The energy is obtained as an interaction between multipoles, generated by quantum source or current fluctuations. The objects' shape and composition enter only through their scattering matrices. The result is exact when all multipoles are included, and converges rapidly. A low frequency expansion yields the energy as a series in the ratio of the objects' size to their separation. As examples, we obtain this series for two spheres with Robin boundary conditions for a scalar field and dielectric spheres for the electromagnetic field. The full interaction at all separations is obtained for spheres with Robin boundary conditions and for perfectly conducting spheres.

Submitted to: *J. Phys. A: Math. Gen.*

1. Introduction

Casimir forces arise when the quantum fluctuations of a scalar, vector, or even fermion field are modified by the presence of static or slowly changing external objects [1]. The objects can be modeled by boundary conditions that they place on the fluctuating field ϕ, by an external field, σ, to which ϕ couples [2], or, in the case of electromagnetism, by a material with space and frequency dependent dielectric and magnetic properties. The Casimir energy is the difference between the energy of the fluctuating field when then objects are present and when the objects are removed to infinite separation.

The advent of precision experimental measurements of Casimir forces [3] and the possibility that they can be applied to nanoscale electromechanical devices [4, 5] has stimulated interest in developing a practical way to calculate the dependence of Casimir energies on the shapes of the objects. Many geometries have been analyzed over the years, but the case of compact objects has proved rather difficult. In a recent Letter we described a new method that makes possible accurate and efficient calculations of Casimir forces and torques between any number of compact objects ‡. The method applies to electromagnetic fields and dielectrics as well as perfect conductors. It also applies to other fields, such as scalar and Dirac, and to any boundary conditions. In this approach, the Casimir energy is given in terms of the fluctuating field's scattering amplitudes from the individual objects, which encode the effects of the shape and boundary conditions. The scattering amplitudes are known analytically in some cases and numerically in others. If the scattering amplitudes are known, then the method can be applied from asymptotically large separation down to separations that are a small fraction of the dimension of the objects. Results at large separations are obtained using low frequency and low angular momentum expansions of scattering amplitudes. The coefficients multiplying the successive orders in inverse separation can be identified with increasingly detailed characteristics of the objects. At small separations the manipulation of large matrices, whose dimensions grow with angular momentum, eventually slows down the calculation. However at these distances other methods, notably the "proximity force approximation" (PFA), apply. Thus it is now possible to obtain an understanding of Casimir forces and torques at all separations for compact objects.

The aim of this talk is to provide a pedagogical introduction to our methods by treating in detail the simplest case, a scalar field obeying a boundary condition on a sharp surface [7]. The complications of electromagnetism and smoothly varying dielectrics were already introduced in Ref. [6] and are discussed here briefly. Our result for the Casimir energy is remarkably simple. For a complex scalar field in the presence of two objects it takes the form,

$$\mathcal{E}_{12}[\mathcal{C}] = \frac{\hbar c}{\pi} \int_0^\infty d\kappa \, \ln\det(\mathbb{I} - \mathbb{T}^1 \mathbb{U}^{12} \mathbb{T}^2 \mathbb{U}^{21}) \,, \tag{1.1}$$

where the determinant is over the partial wave indices on transition matrices $\mathbb{T}^\alpha$ and translation matrices $\mathbb{U}^{\alpha\beta}$ and the integral is over $\kappa = -i\omega/c$, the imaginary wavenumber. For a (real) electromagnetic field the result has the same form with an additional factor of 1/2 and the appropriate matrices for scattering and propagation of electromagnetic waves. In Sections 4 and 5 the usefulness of this result is demonstrated through several specific applications for scalar and electromagnetic fields, respectively.

The force between atoms at asymptotically large distances was computed by Casimir and Polder [8] and related to the atoms' polarizabilities. For compact objects, such as two spheres, Feinberg and Sucher [9] generalized this work to include magnetic effects. Earlier studies of the Casimir force between compact objects include a multiple reflection formalism [10], which in principle could be applied to perfect conductors of arbitrary shape. A formulation of the Casimir energy of compact objects in terms of their scattering matrices, for a scalar field coupled to a dielectric background, is introduced in Ref. [11], where it is suggested that it can also be extended to the EM case.

---

‡ This presentation is based on work performed in collaboration with N. Graham and M. Kardar. For a complete exposition, see Refs. [6] and [7].

Recently Gies et al. [12] used numerical methods to evaluate the Casimir force between two Dirichlet spheres for a scalar field, over a range of subasymptotic separations, and in other open geometries such as a plate and a cylinder [13] or finite plates with edges [14]. Bulgac and collaborators [15] applied scattering theory methods to the same scalar Dirichlet problem and obtained results over a wide range of separations. The only explicit calculations for subasymptotic distances up to now have been for a scalar field obeying Dirichlet boundary conditions on two spheres, a sphere and a plate [15] and for electromagnetic fields for a plate and a cylinder [16] and two perfectly conducting spheres [6].

2. Casimir energy from functional integral: Scalar field

In this Section we review formalism essential for our work that is based on the functional integral approach of Refs. [17, 18, 19].

2.1. Functional integral formulation

We consider a complex quantum field, $\phi(\mathbf{x},t)$, which is defined over all space and constrained by boundary conditions $\mathcal{C}$ on a set of fixed surfaces Σ_α, for $\alpha = 1, 2, \ldots, N$, but is otherwise non-interacting. We assume that the surfaces are closed and compact and refer to their interiors as "objects." Our starting point is the functional integral representation for the trace of the propagator, $\operatorname{Tr} e^{-iH_{\mathcal{C}}T/\hbar}$ [20],

$$\operatorname{Tr} e^{-iH_{\mathcal{C}}T/\hbar} = \int \left[\mathcal{D}\phi\right]_{\mathcal{C}} \, e^{\frac{i}{\hbar}S_E[\phi]} \; \equiv \; Z\left[\mathcal{C}\right], \tag{2.1}$$

where the subscript $\mathcal{C}$ denotes the constraints imposed by the boundary conditions.§ The integral is over all field configurations that obey the boundary conditions and are periodic in a time interval T. $S[\phi]$ is the action for a free complex field,

$$S_E[\phi] = \int_0^T dt \int d\mathbf{x} \, \left(\frac{1}{c^2}|\partial_t\phi|^2 - |\nabla\phi|^2\right), \tag{2.2}$$

where the $\mathbf{x}$-integration covers all space.‖

The ground state energy can be projected out of the trace in Eq. (2.1) by setting $T = -i\Lambda/c$ taking the limit $\Lambda \to \infty$,

$$\mathcal{E}_0[\mathcal{C}] = -\lim_{\Lambda\to\infty} \frac{\hbar c}{\Lambda} \ln\left(\operatorname{Tr} e^{-H_{\mathcal{C}}\Lambda/\hbar c}\right) = -\lim_{T\to\infty} \frac{\hbar c}{\Lambda} \ln Z[\mathcal{C}]\,, \tag{2.3}$$

---

§ We have used an abbreviated notation for the functional integral. Since ϕ is complex $\int \mathcal{D}\phi$ should be understood as $\int \mathcal{D}\phi\mathcal{D}\phi^*$, and similarly in subsequent functional integrals.

‖ Note that ϕ is defined and can fluctuate inside the objects bounded by the surfaces Σ_α. In this feature our formalism departs from some treatments where the field is defined to be strictly zero (for Dirichlet boundary conditions) inside the objects. The fluctuations interior to the objects do not depend on the separations between them and therefore do not affect Casimir forces or torques.

and the Casimir energy is obtained by subtracting the ground state energy when the objects have been removed to infinite separation,

$$\mathcal{E}[\mathcal{C}] = -\lim_{\Lambda\to\infty} \frac{\hbar c}{\Lambda} \ln\left(Z[\mathcal{C}]/Z_\infty\right) . \tag{2.4}$$

In the standard formulation, the constraints are implemented by boundary conditions on the field ϕ at the surfaces $\{\Sigma_\alpha\}$. The usual choices are Dirichlet, $\phi = 0$, Neumann, $\partial_n\phi = 0$, or mixed (Robin), $\phi - \lambda\partial_n\phi = 0$, where ∂_n is the normal derivative pointing out of the objects. To be specific, we first consider Dirichlet boundary conditions. The extension to the Neumann case is presented in Ref [7]. As noted in the Introduction, the only effect of the choice of boundary conditions is to determine which $\mathbb{T}$-matrix appears in the functional determinant, Eq. (1.1).

Since the constraints on ϕ are time independent, the integral over $\phi(\mathbf{x}, t)$ may be written as an infinite product of integrals over Fourier components,

$$\int [\mathcal{D}\phi]_{\mathcal{C}} = \prod_{n=-\infty}^{\infty} [\mathcal{D}\phi_n(\mathbf{x})]_{\mathcal{C}} , \tag{2.5}$$

where

$$\phi(\mathbf{x}, t) = \sum_{n=-\infty}^{\infty} \phi_n(\mathbf{x}) e^{2\pi int/T}, \tag{2.6}$$

and the logarithm of Z becomes a sum,

$$\ln Z[\mathcal{C}] = \sum_{n=-\infty}^{\infty} \ln \left\{ \int [\mathcal{D}\phi_n(\mathbf{x})]_{\mathcal{C}} \exp\left[i\frac{T}{\hbar} \int d\mathbf{x} \left(\left(\frac{2\pi n}{cT}\right)^2 |\phi_n(\mathbf{x})|^2 - |\nabla\phi_n(\mathbf{x})|^2 \right)\right]\right\} . \tag{2.7}$$

As $T \to \infty$, $\sum_n$ can be replaced by $\frac{cT}{2\pi}\int_{-\infty}^{\infty} dk$, where $k = 2\pi n/(cT)$ and $\phi_n(\mathbf{x})$ is replaced by $\phi(\mathbf{x}, k)$. Combining the positive and negative k-integrals gives

$$\begin{aligned} \ln Z[\mathcal{C}] &= \frac{cT}{\pi} \int_0^\infty dk \ln \left\{ \int [\mathcal{D}\phi(\mathbf{x}, k)]_{\mathcal{C}} \exp\left[i\frac{T}{\hbar} \int d\mathbf{x} \left(k^2 |\phi(\mathbf{x}, k)|^2 - |\nabla\phi(\mathbf{x}, k)|^2 \right)\right]\right\} \\ &= \frac{cT}{\pi} \int_0^\infty dk \ln \mathfrak{Z}_{\mathcal{C}}(k) , \end{aligned} \tag{2.8}$$

where

$$\mathfrak{Z}_{\mathcal{C}}(k) = \int [\mathcal{D}\phi(\mathbf{x}, k)]_{\mathcal{C}} \exp\left[i\frac{T}{\hbar} \int d\mathbf{x} \left(k^2 |\phi(\mathbf{x}, k)|^2 - |\nabla\phi(\mathbf{x}, k)|^2 \right)\right] , \tag{2.9}$$

is the functional integral at fixed k.

To extract the Casimir energy, we use $T = -i\Lambda/c$ and Wick rotate the k-integration ($k = i\kappa$ with $\kappa > 0$). ¶ Using Eq. (2.4), we obtain,

$$\mathcal{E}[\mathcal{C}] = -\frac{\hbar c}{\pi} \int_0^\infty d\kappa \ln \frac{\mathfrak{Z}_{C}(i\kappa)}{\mathfrak{Z}_\infty(i\kappa)} . \tag{2.10}$$

¶ A more careful treatment of the rotation of the integration contour to the imaginary axis is necessary in the presence of bound states.

Here $\mathfrak{Z}_{\mathcal{C}}(i\kappa)$ is given by the Euclidean functional integral,

$$\mathfrak{Z}_{\mathcal{C}}(i\kappa) = \int [\mathcal{D}\phi(\mathbf{x}, i\kappa)]_{\mathcal{C}} \exp\left[-\frac{T}{\hbar}\int d\mathbf{x}\left(\kappa^2|\phi(\mathbf{x}, i\kappa)|^2 + |\nabla\phi(\mathbf{x}, i\kappa)|^2\right)\right]. \tag{2.11}$$

It remains to incorporate the constraints directly into the functional integral using the methods of Refs. [21, 17]. Working in Minkowski space, we consider the fixed frequency functional integral, $\mathfrak{Z}_{\mathcal{C}}(k)$ (and suppress the label k on the field ϕ). Following Ref. [21, 17], we implement the constraints in the functional integral by means of a functional δ-function. For Dirichlet boundary conditions the constraint reads,

$$\int [\mathcal{D}\phi(\mathbf{x})]_{\mathcal{C}} = \int [\mathcal{D}\phi(\mathbf{x})] \prod_{\alpha=1}^{N} \int [\mathcal{D}\varrho_\alpha(\mathbf{x})] \exp\left[i\frac{T}{\hbar}\int_{\Sigma_\alpha} d\mathbf{x}\left(\varrho_\alpha^*(\mathbf{x})\phi(\mathbf{x}) + \text{c.c.}\right)\right], \tag{2.12}$$

where the functional integration over ϕ is no longer constrained. Other boundary conditions can be implemented similarly. In the resulting functional integral,

$$\begin{aligned}\mathfrak{Z}_{\mathcal{C}}(k) = & \prod_{\alpha=1}^{N}\int [\mathcal{D}\varrho_\alpha(\mathbf{x})] \int [\mathcal{D}\phi(\mathbf{x})] \exp\left[i\frac{T}{\hbar}\left(\int d\mathbf{x}\left(k^2|\phi(\mathbf{x})|^2 - |\nabla\phi(\mathbf{x})|^2\right)\right.\right. \\ & + \left.\left.\sum_\alpha \int_{\Sigma_\alpha} d\mathbf{x}\left(\varrho_\alpha^*(\mathbf{x})\phi(\mathbf{x}) + \text{c.c.}\right)\right)\right] \\ \equiv & \prod_{\alpha=1}^{N}\int [\mathcal{D}\varrho_\alpha(\mathbf{x})] \int [\mathcal{D}\phi(\mathbf{x})] \exp\left(i\frac{T}{\hbar}\widetilde{S}[\phi, \varrho]\right),\end{aligned} \tag{2.13}$$

the fields fluctuate without constraint throughout space and the sources $\{\varrho_\alpha\}$ fluctuate on the surfaces. We denote the new "effective action" including both the fields and sources by $\widetilde{S}[\phi, \varrho]$.

2.2. Performing the integral over ϕ

We start with the expression for the fixed-k functional integral, Eq. (2.13). For any fixed sources, $\{\varrho_\alpha\}$, there is a unique classical field, $\phi_{\text{cl}}[\varrho]$, that is the solution to $\delta\widetilde{S}[\phi, \varrho]/\delta\phi(\mathbf{x}) = 0$. The classical theory defined by $\widetilde{S}[\phi, \varrho]$, describes a complex scalar field coupled to a set of sources on the surfaces, and is a generalization of electrostatics. By analogy with electrostatics, the field ϕ is continuous throughout space, but its normal derivative jumps by $\varrho_\alpha(\mathbf{x})$ across Σ_a. Indeed, the classical equations of motion that follow from $\delta\widetilde{S}/\delta\phi = 0$ are

$$\begin{aligned}&\left(\nabla^2 + k^2\right)\phi_{\text{cl}}(\mathbf{x}) &&= 0, \quad \text{for } \mathbf{x} \notin \Sigma_\alpha, \\ &\Delta\phi_{\text{cl}}(\mathbf{x}) &&= 0, \quad \text{for } \mathbf{x} \in \Sigma_\alpha, \\ &\Delta\partial_n\phi_{\text{cl}}|_{\mathbf{x}} &&= \varrho_\alpha(\mathbf{x}), \quad \text{for } \mathbf{x} \in \Sigma_\alpha,\end{aligned} \tag{2.14}$$

where $\Delta\phi = \phi_{\text{in}} - \phi_{\text{out}}$ and $\Delta\partial_n\phi = \partial_n\phi|_{\text{in}} - \partial_n\phi_{\text{out}}$. The subscripts "in" and "out" refer to the field inside and outside the bounding surface Σ_α. As before, all normals point out of the compact surfaces. The solution to Eq. (2.14) is unique up to solutions of the homogeneous equations, which we exclude by demanding that $\phi_{\rm cl}$ vanish when the $\{\varrho_\alpha\} = 0$. Continuing the analogy with electrostatics, we can write the classical field in terms of the free Green's function and the sources,

$$\phi_{\rm cl}(\mathbf{x}) = \sum_\beta \int_{\Sigma_\beta} d\mathbf{x}' \mathcal{G}_0(\mathbf{x}, \mathbf{x}', k) \varrho_\beta(\mathbf{x}') \,, \tag{2.15}$$

where the free Green's function is given by

$$\begin{aligned} \mathcal{G}_0(\mathbf{x}, \mathbf{x}', k) \equiv \frac{e^{ik|\mathbf{x}-\mathbf{x}'|}}{4\pi|\mathbf{x}-\mathbf{x}'|} &= ik \sum_{lm} j_l(kr_<) h_l^{(1)}(kr_>) Y_{lm}(\hat{\mathbf{x}}) Y_{lm}^*(\hat{\mathbf{x}}') \\ &= ik \sum_{lm} j_l(kr_<) h_l^{(1)}(kr_>) Y_{lm}(\hat{\mathbf{x}}') Y_{lm}^*(\hat{\mathbf{x}}) \,, \end{aligned} \tag{2.16}$$

where the notations $r_{<(>)}$ refer to whichever of r, r' is the smaller (larger).

To compute the functional integral over ϕ, we first decompose ϕ into the classical part given by Eq. (2.15) and a fluctuating part,

$$\phi(\mathbf{x}) = \phi_{\rm cl}(\mathbf{x}) + \delta\phi(\mathbf{x}) \,. \tag{2.17}$$

Then, because the effective action, $\widetilde{S}$, is quadratic in ϕ, the $\delta\phi$ dependent terms are independent of $\phi_{\rm cl}$,

$$\mathfrak{Z}_{\mathcal{C}}(k) = \prod_{\alpha=1}^{N} \int [\mathcal{D}\varrho_\alpha(\mathbf{x})] \, e^{i\frac{T}{\hbar}\widetilde{S}_{\rm cl}[\varrho]} \int [\mathcal{D}\delta\phi(\mathbf{x})] \exp\left[i\frac{T}{\hbar} \int d\mathbf{x} \left(k^2 |\delta\phi(\mathbf{x})|^2 - |\nabla\delta\phi(\mathbf{x})|^2 \right) \right] . \tag{2.18}$$

The classical action can be simplified by using the equations of motion, Eq. (2.14), which make it possible to express the action entirely in terms of integrals over the surfaces $\{\Sigma_\alpha\}$,

$$\widetilde{S}_{\rm cl}[\varrho] = \frac{1}{2} \sum_\alpha \int_{\Sigma_\alpha} d\mathbf{x} \, \left(\varrho_\alpha^*(\mathbf{x}) \phi_{\rm cl}(\mathbf{x}) + \text{c.c.} \right) \,, \tag{2.19}$$

where $\phi_{\rm cl}(\mathbf{x})$ is understood to be a functional of the sources ϱ_α.

The functional integral over $\delta\phi$ is *independent of the classical field* $\phi_{\rm cl}$ and defines the energy of the unconstrained vacuum fluctuations of ϕ. This term is divergent, or, more precisely, depends on some unspecified ultraviolet cutoff. However it can be discarded because it is independent of the sources and therefore common to $\mathfrak{Z}_{\mathcal{C}}$ and $\mathfrak{Z}_\infty$. Note that this result is an explicit demonstration of the contention of Ref. [22]: the Casimir force has nothing to do with the *vacuum* fluctuations of ϕ, but is instead a consequence of the interaction between fluctuating sources in the materials. It is therefore not directly relevant to the fluctuations that are conjectured to be associated with the dark energy.

From Eq. (2.15) it is clear that the solution to Eq. (2.14) obeys the superposition principle: $\phi_{\rm cl}(\mathbf{x})$ is a sum of contributions from each of the sources,

$$\phi_{\rm cl}(\mathbf{x}) = \sum_\beta \phi_\beta(\mathbf{x}) \,, \tag{2.20}$$

where ϕ_β satisfies Eq. (2.14) with all sources set equal to zero except for ϱ_β. So the action can be expressed as a double sum over surfaces and over contributions to ϕ_{cl} generated by different objects. This leaves a partition function, $\mathfrak{Z}_{\mathcal{C}}(k)$, of the form

$$\mathfrak{Z}_{\mathcal{C}}(k) = \prod_{\alpha=1}^{N} \int [\mathcal{D}\varrho_\alpha(\mathbf{x})] \exp\left[\frac{i}{2}\frac{T}{\hbar}\sum_{\alpha,\beta}\int_{\Sigma_\alpha} d\mathbf{x}\,(\varrho_\alpha^*(\mathbf{x})\phi_\beta(\mathbf{x}) + \text{c.c.}\,)\right], \tag{2.21}$$

to be evaluated.

2.3. Evaluation of the Classical Action

The classical action in Eq. (2.21) contains two qualitatively different terms, the interaction between different sources, $\alpha \neq \beta$, and the self-interaction of the source ϱ_α. Both can be expressed as functions of the multipole moments of the sources on the surfaces.

2.3.1. Interaction terms: $\alpha \neq \beta$ Consider the contribution to the action from the field, ϕ_β, generated by the source, ϱ_β, integrated over the surface Σ_α,

$$\widetilde{S}_{\beta\alpha} = \frac{1}{2}\int_{\Sigma_\alpha} d\mathbf{x}_\alpha\,(\varrho_\alpha^*(\mathbf{x}_\alpha)\phi_\beta(\mathbf{x}_\alpha) + \text{c.c.}\,)\,, \tag{2.22}$$

where the subscript α on $\mathbf{x}_\alpha$ indicates that the integration runs over coordinates measured relative to the origin of object α. The field $\phi_\beta(\mathbf{x}_\beta)$, *measured relative to the origin of object* β, can be represented as an integral over its sources on the surface Σ_β as in Eq. (2.15). Since every point on Σ_α is outside of a sphere enclosing Σ_β, the partial wave representation of $\mathcal{G}_0$ simplifies. The coordinate $\mathbf{x}_>$ is always associated with $\mathbf{x}_\beta$ and $\mathbf{x}_<$ is identified with $\mathbf{x}'_\beta$, so Eq. (2.15) can be written

$$\phi_\beta(\mathbf{x}_\beta) = ik\sum_{lm} h_l^{(1)}(kr_\beta)Y_{lm}(\hat{\mathbf{x}}_\beta)\int_{\Sigma_\beta} d\mathbf{x}'_\beta j_l(kr'_\beta)Y^*_{lm}(\hat{\mathbf{x}}'_\beta)\varrho_\beta(\mathbf{x}'_\beta)\,. \tag{2.23}$$

Note that the arguments of the Bessel functions and spherical harmonics are all defined relative to the origin $\mathcal{O}_\beta$. In particular, r'_β and $\hat{\mathbf{x}}'_\beta$ are the radial and angular coordinates relative to $\mathcal{O}_\beta$ corresponding to a point $\mathbf{x}'$ on the surface Σ_β. The integrals over Σ_β define the *multipole moments* of the source ϱ_β, which will be our final quantum variables,

$$Q_{\beta,lm} \equiv \int_{\Sigma_\beta} d\mathbf{x}_\beta j_l(kr_\beta)Y^*_{lm}(\hat{\mathbf{x}}_\beta)\varrho_\beta(\mathbf{x}_\beta), \tag{2.24}$$

so that

$$\phi_\beta(\mathbf{x}_\beta) = ik\sum_{lm} Q_{\beta,lm}h_l^{(1)}(kr_\beta)Y_{lm}(\hat{\mathbf{x}}_\beta). \tag{2.25}$$

The field ϕ_β viewed from the surface Σ_α is a superposition of solutions to the Helmholtz equation that are regular at the origin $\mathcal{O}_\alpha$. Using translation formulas, summarized in Ref. [23], the field generated by object Σ_β can be written as function of the coordinate $\mathbf{x}_\alpha$, measured from the origin $\mathcal{O}_\alpha$, as

$$\phi_\beta(\mathbf{x}_\alpha) = ik \sum_{lm} Q_{\beta,lm} \sum_{l'm'} \mathcal{U}^{\alpha\beta}_{l'm'lm} j_{l'}(kr_\alpha) Y_{l'm'}(\hat{\mathbf{x}}_\alpha) \,. \tag{2.26}$$

The matrices $\mathcal{U}^{\alpha\beta}_{l'm'lm}$ are shape and boundary condition independent and represent the interaction between the multipoles. This result, in turn, can be substituted into the contribution $\widetilde{S}_{\beta\alpha}$ to the action, leading to the simple result

$$\widetilde{S}_{\beta\alpha}[Q_\alpha, Q_\beta] = \frac{ik}{2} \sum_{lml'm'} Q^*_{\alpha,l'm'} \mathcal{U}^{\alpha\beta}_{l'm'lm} Q_{\beta,lm} + \text{c.c.} \,. \tag{2.27}$$

Note that the contributions to the action that couple fields and sources on different objects make no reference to the particular boundary conditions that characterize the Casimir problem. They depend only on the multipole moments of the fields and on the geometry through the translation matrix $\mathbb{U}^{\alpha\beta}$.

2.3.2. Self-interaction terms We turn to the terms in $\widetilde{S}_{\text{cl}}$ where the field and the source both refer to the same surface, Σ_α:

$$\widetilde{S}_\alpha[\varrho_\alpha] = \frac{1}{2} \int_{\Sigma_\alpha} d\mathbf{x} \left(\varrho^*_\alpha(\mathbf{x}) \phi_\alpha(\mathbf{x}) + \text{c.c.} \right) \,. \tag{2.28}$$

For the self-interactions terms, we only use the coordinate system with origin $\mathcal{O}_\alpha$ inside the surface Σ_α, and hence drop the label α on the coordinates in this section. Since $\phi_\alpha(\mathbf{x})$ is continuous across the surface, we can regard the ϕ_α in Eq. (2.28) as the field *inside* Σ_α, $\phi_{\text{in},\alpha}$, which is a solution to Helmholtz's equation that must be regular at the origin $\mathcal{O}_\alpha$,

$$\phi_{\text{in},\alpha}(\mathbf{x}) = \sum_{lm} \phi_{\alpha,lm} j_l(kr) Y_{lm}(\hat{\mathbf{x}}) \,. \tag{2.29}$$

Substituting this expansion into Eq. (2.28), we obtain

$$\widetilde{S}_\alpha[\varrho_\alpha] = \frac{1}{2} \sum_{lm} \left(\phi_{\alpha,lm} Q^*_{\alpha,lm} + \text{c.c.} \right) \,, \tag{2.30}$$

where the $Q_{\alpha,lm}$ are the multipole moments of the sources, defined in the previous subsection.

Finally we relate $\phi_{\alpha,lm}$ back to the multipole moments of the source to get an action entirely in terms of the $Q_{\alpha,lm}$. The field $\phi_{\alpha,\text{out}}$ at points *outside* of Σ_α obeys Helmholtz's equation and must equal $\phi_{\alpha,\text{in}}$ on the surface S. Therefore it can be written as $\phi_{\alpha,\text{in}}$ *plus a superposition of the regular solutions to the Helmholtz equation that vanish on* Σ_α,

$$\begin{aligned} \phi_{\alpha,\text{out}}(\mathbf{x}) &= \phi_{\alpha,\text{in}}(\mathbf{x}) + \Delta\phi_\alpha(\mathbf{x}) \\ &= \phi_{\alpha,\text{in}}(\mathbf{x}) + \sum_{lm} \chi_{\alpha,lm} \left(j_l(kr) Y_{lm}(\hat{\mathbf{x}}) + \sum_{l'm'} \mathcal{T}^\alpha_{l'm'lm}(k) h^{(1)}_{l'}(kr) Y_{l'm'}(\hat{\mathbf{x}}) \right) \,. \end{aligned} \tag{2.31}$$

The second term, $\Delta\phi_\alpha$, vanishes on Σ_α because $\mathbb{T}^\alpha$ is the scattering amplitude for the Dirichlet problem.

The field we seek is generated in response to the sources and therefore falls exponentially (for k with positive imaginary part) as $r \to \infty$. Therefore the terms in Eq. (2.31) that are proportional to $j_l(kr)$ must cancel. Comparing Eq. (2.31) with Eq. (2.29), we conclude that $\chi_{\alpha,lm} = -\phi_{\alpha,lm}$, and therefore

$$\phi_{\alpha,\text{out}}(\mathbf{x}) = -\sum_{lm} \phi_{\alpha,lm} \sum_{l'm'} \mathcal{T}^\alpha_{l'm'lm}(k) h^{(1)}_{l'}(kr) Y_{l'm'}(\hat{\mathbf{x}})\,. \tag{2.32}$$

On the other hand, $\phi_{\alpha,\text{out}}(\mathbf{x})$ can be expressed as an integral over the source as in Eq. (2.15),

$$\phi_{\alpha,\text{out}}(\mathbf{x}) = \int_{\Sigma_\alpha} d\mathbf{x}' \mathcal{G}_0(\mathbf{x}, \mathbf{x}', k) \varrho_\alpha(\mathbf{x}')\,. \tag{2.33}$$

Using the partial wave expansion for the free Green's function, Eq. (2.16), we find

$$\phi_{\alpha,\text{out}}(\mathbf{x}) = ik \sum_{l'm'} Q_{\alpha,l'm'} h^{(1)}_{l'}(kr) Y_{l'm'}(\hat{\mathbf{x}}), \tag{2.34}$$

and comparing with Eq. (2.32), we see that

$$ikQ_{\alpha,l'm'} = -\sum_{lm} \mathcal{T}^\alpha_{l'm'lm}(k)\phi_{\alpha,lm},$$

or

$$\phi_{\alpha,lm} = -ik \sum_{l'm'} [\mathcal{T}^\alpha]^{-1}_{lml'm'} Q_{\alpha,l'm'}, \tag{2.35}$$

where $[\mathbb{T}^\alpha]^{-1}$ is the inverse of the Dirichlet transition matrix $\mathbb{T}^\alpha$. When this is combined with Eq. (2.30), we obtain the desired expression for the self-interaction contribution to the action,

$$\widetilde{S}_\alpha[Q_\alpha] = -\frac{ik}{2} \sum_{lml'm'} Q^*_{\alpha,lm} [\mathcal{T}^\alpha]^{-1}_{lml'm'} Q_{\alpha,l'm'} + \text{c.c.}\ . \tag{2.36}$$

2.4. Evaluation of the Integral over Sources

Combining Eq. (2.36) with Eq. (2.27), we obtain an expression for the action that is a quadratic functional of the multipole moments of the sources on the surfaces. The functional integral Eq. (2.21) can be evaluated by changing variables from the sources, $\{\varrho_\alpha\}$ to the multipole moments. The functional determinant that results from this change of variables can be discarded because it is a common factor which cancels between $\mathfrak{Z}_\mathcal{C}$ and $\mathfrak{Z}_\infty$. To compute the functional integral we analytically continue to imaginary frequency, $k = i\kappa$, $\kappa > 0$,

$$\mathfrak{Z}_\mathcal{C}(i\kappa) = \prod_{\alpha=1}^{N} \int [\mathcal{D}Q_\alpha \mathcal{D}Q^*_\alpha] \exp\left\{ -\frac{\kappa}{2}\frac{T}{\hbar} \sum_\alpha Q^*_\alpha [\mathbb{T}^\alpha]^{-1} Q_\alpha + \frac{\kappa}{2}\frac{T}{\hbar} \sum_{\alpha\neq\beta} Q^*_\alpha \mathbb{U}^{\alpha\beta} Q_\beta + \text{c.c.} \right\}, \tag{2.37}$$

where we have suppressed the partial wave indices. The functional integral Eq. (2.37) yields the inverse determinant of a matrix $\mathbb{M}_{\mathcal{C}}^{\alpha\beta}$ that is composed of the inverse transition matrices $[\mathbb{T}^{\alpha}]^{-1}$ on its diagonal and the translation matrices $\mathbb{U}^{\alpha\beta}$ on the off-diagonals:

$$\mathbb{M}_{\mathcal{C}}^{\alpha\beta} = [\mathbb{T}^{\alpha}]^{-1}\delta_{\alpha\beta} - \mathbb{U}^{\alpha\beta}(1-\delta_{\alpha\beta})\,. \tag{2.38}$$

Finally we substitute into Eq. (2.10) to obtain the Casimir energy,

$$\mathcal{E}[\mathcal{C}] = \frac{\hbar c}{\pi}\int_0^\infty d\kappa \ln \frac{\det \mathbb{M}_{\mathcal{C}}(i\kappa)}{\det \mathbb{M}_{\infty}(i\kappa)}\,, \tag{2.39}$$

where the determinant is taken with respect to the partial wave indices and the object indices α, β, and $\mathbb{M}_{\infty}^{\alpha\beta} = [\mathbb{T}^{\alpha}]^{-1}\delta_{\alpha\beta}$ is the result of removing the objects to infinite separation, where the interaction effects vanish.

In the special case of two interacting objects Eq. (2.39) simplifies to

$$\mathcal{E}_2[\mathcal{C}] = \frac{\hbar c}{\pi}\int_0^\infty d\kappa \ln\det(1-\mathbb{T}^1\mathbb{U}^{12}\mathbb{T}^2\mathbb{U}^{21})\,, \tag{2.40}$$

where $\mathbb{T}^{\alpha}, \alpha = 1, 2$, and $\mathbb{U}^{\alpha\beta}$ are the transition and translation matrices for the two objects.

3. Casimir energy from functional integral: Electromagnetic field

In this section we provide a brief description of the generalization of the concepts from the previous section to electromagnetic fields [6]. Here we start directly with a formulation in terms of sources, the current and charge densities $\mathbf{J}$, ϱ. Using that the EM gauge and scalar potential $[A(\mathbf{x},t), \Phi(\mathbf{x},t)]$ are given by

$$[\mathbf{A}(\mathbf{x}), \Phi(\mathbf{x})] = \int d\mathbf{x}'\, G_0(\mathbf{x},\mathbf{x}')[\mathbf{J}(\mathbf{x}'), \varrho(\mathbf{x}')]\;, \tag{3.1}$$

where now $G_0(\mathbf{x},\mathbf{x}') = e^{ik|\mathbf{x}-\mathbf{x}'|}/(4\pi|\mathbf{x}-\mathbf{x}'|)$, the action $S[\mathbf{J}] = \int (dk/4\pi)(S_k[\mathbf{J}] + S_k^*[\mathbf{J}])$ for the currents densities, defined inside the objects, can be written as

$$S_k[\{\mathbf{J}_\alpha\}] = \frac{1}{2}\int d\mathbf{x}\, d\mathbf{x}' \sum_{\alpha\beta} \mathbf{J}_\alpha^*(\mathbf{x})\, \mathcal{G}_0(\mathbf{x},\mathbf{x}')\, \mathbf{J}_\beta(\mathbf{x}')\,, \tag{3.2}$$

where $\mathcal{G}_0(\mathbf{x},\mathbf{x}') = G_0(\mathbf{x},\mathbf{x}') - \frac{1}{k^2}\nabla\otimes\nabla' G_0(\mathbf{x},\mathbf{x}')$ is the tensor Green's function. This is the analogous expression to the one for a scalar field in Eq. (2.21) with the solution of Eq. (2.15) substituted. Next we must constrain the currents to be *induced* sources that depend on shape and material of the objects. Formally this is achieved by integrating over currents, inserting constraints to ensure that the currents in vacuum simulate the correct induction of microscopic polarization $\mathbf{P}_\alpha$ and magnetization $\mathbf{M}_\alpha$ (from all multipoles) inside the dielectric objects in response to an incident wave.

Let us consider one object. First, the induced current is $\mathbf{J}_\alpha = -ik\mathbf{P}_\alpha + \nabla \times \mathbf{M}_\alpha$, and since $\mathbf{P}_\alpha = (\epsilon_\alpha - 1)\mathbf{E}$, $\mathbf{M}_\alpha = (1 - 1/\mu_\alpha)\mathbf{B}$, it can be expressed in terms of the total fields $\mathbf{E}$, $\mathbf{B}$ inside the object as

$$\mathbf{J}_\alpha = -ik(\epsilon_\alpha - 1)\mathbf{E} + \nabla \times [(1 - 1/\mu_\alpha)\mathbf{B}] \,. \tag{3.3}$$

Second, the total field inside the object must consist of the field generated by $\mathbf{J}_\alpha$ and the incident field $\mathbf{E}_0(\{\mathbf{J}_\alpha, \mathbb{S}^\alpha\}, \mathbf{x})$ that has to impinge on the object to induce $\mathbf{J}_\alpha$, so that

$$\mathbf{E}(\mathbf{x}) = \mathbf{E}_0(\{\mathbf{J}_\alpha, \mathbb{S}^\alpha\}, \mathbf{x}) + ik \int d\mathbf{x}' \, \mathcal{G}_0(\mathbf{x}, \mathbf{x}') \, \mathbf{J}_\alpha(\mathbf{x}') \,. \tag{3.4}$$

The incident field depends on the current density to be induced and on the scattering matrix $\mathbb{S}^\alpha$ of the object, which connects the incident wave to the scattered wave. It is fully specified by the multipole moments of $\mathbf{J}_\alpha$ (see below for details). Substituting Eq. (3.4) and $\mathbf{B} = (1/ik)\nabla \times \mathbf{E}$ into Eq. (3.3) yields a self-consistency condition that constrains the current $\mathbf{J}_\alpha$. If one writes this condition as $\mathcal{C}_\alpha[\mathbf{J}_\alpha] = 0$ for each object, the functional integration over the currents constrained this way for all objects yields the partition function

$$\mathcal{Z} = \int \prod_\alpha \mathcal{D}\mathbf{J}_\alpha \prod_{\mathbf{x} \in V_\alpha} \delta(\mathcal{C}_\alpha[\mathbf{J}_\alpha(\mathbf{x})]) \exp\left(iS[\{\mathbf{J}_\alpha\}]\right) \,. \tag{3.5}$$

It is instructive to look at two compact objects at a distance d, measured between the (arbitrary) origins $\mathcal{O}_\alpha$ inside the objects. In this case the action of Eq. (3.2) is

$$\begin{aligned} S_k[\{\mathbf{J}_\alpha\}] = {} & \frac{1}{2} \sum_{\alpha \neq \beta} \int d\mathbf{x}_\alpha \, \mathbf{J}^*_\alpha(\mathbf{x}_\alpha) \frac{1}{ik} \mathbf{E}_\beta(\mathbf{x}_\alpha - d_\alpha \hat{\mathbf{z}}) \\ & + \frac{1}{2} \sum_\alpha \int d\mathbf{x}_\alpha d\mathbf{x}'_\alpha \, \mathbf{J}^*_\alpha(\mathbf{x}_\alpha) \, \mathcal{G}_0(\mathbf{x}_\alpha, \mathbf{x}'_\alpha) \, \mathbf{J}_\alpha(\mathbf{x}'_\alpha) \,, \end{aligned} \tag{3.6}$$

where we have substituted the electric field $\mathbf{E}_\alpha(\mathbf{x}_\alpha) = ik \int d\mathbf{x}'_\alpha \, \mathcal{G}_0(\mathbf{x}_\alpha, \mathbf{x}'_\alpha) \, \mathbf{J}_\alpha(\mathbf{x}'_\alpha)$ and the fields are measured now in local coordinates so that $\mathbf{x} = \mathcal{O}_\alpha + \mathbf{x}_\alpha$, and $d_\alpha = d$ $(-d)$ for $\alpha = 1(2)$. The off-diagonal terms in Eq. (3.6) represent the interaction between the currents on the two materials. A natural way to decompose the interaction between charges is to use the multipole expansion. For each body we define magnetic and electric multipoles as

$$\begin{aligned} Q^\alpha_{\mathrm{M},lm} &= \frac{k}{\lambda} \int d\mathbf{x}_\alpha \, \mathbf{J}_\alpha(\mathbf{x}_\alpha) \nabla \times [\mathbf{x}_\alpha j_l(kr_\alpha) Y^*_{lm}(\hat{\mathbf{x}}_\alpha)] \\ Q^\alpha_{\mathrm{E},lm} &= \frac{1}{\lambda} \int d\mathbf{x}_\alpha \, \mathbf{J}_\alpha(\mathbf{x}_\alpha) \nabla \times \nabla \times [\mathbf{x}_\alpha j_l(kr_\alpha) Y^*_{lm}(\hat{\mathbf{x}}_\alpha)] \,, \end{aligned} \tag{3.7}$$

for $l \geq 1$, $|m| \leq l$, where $\lambda = \sqrt{l(l+1)}$, j_l are spherical Bessel functions and Y_{lm} spherical harmonics. We change variables from currents to multipoles in the functional integral and, as the final step in our quantization, integrate over all multipole fluctuations on the two objects weighted by the effective action,

$$S_k^{\rm eff}[\{Q^\alpha_{lm}\}] = \frac{1}{2}\frac{i}{k}\sum_{lml'm'}\left\{Q^{1*}_{lm}\,U^{12}_{lml'm'}\,Q^2_{l'm'}+Q^{2*}_{lm}\,U^{21}_{lml'm'}\,Q^1_{l'm'}+\sum_{\alpha=1,2}Q^{\alpha*}_{lm}\,[-T^\alpha]^{-1}_{lml'm'}\,Q^\alpha_{l'm'}\right\}, \tag{3.8}$$

with $Q^\alpha_{lm} = (Q^\alpha_{{\rm M},lm}, Q^\alpha_{{\rm E},lm})$. Formally, this action resembles that for a scalar field. The vector nature of the EM field is reflected by the presence of two different polarizations and corresponding electric and magnetic multipoles. Let us discuss the terms appearing in Eq. (3.8) and sketch its derivation.

Off-diagonal terms — We need to know the electric fields in Eq. (3.6) exterior to the source that generates them. They can be represented in terms of the multipoles as $\mathbf{E}_\beta(\mathbf{x}_\beta) = -k\sum_{lm} Q^\beta_{lm}\mathbf{\Psi}^{\rm out}_{lm}(\mathbf{x}_\beta)$ where $\mathbf{\Psi}^{\rm out}_{lm}(\mathbf{x}_\beta)$ are *outgoing* vector solutions of the Helmholtz equation in the coordinates of object β[+]. We would like to express the currents $\mathbf{J}^*_\alpha$ in Eq. (3.6) also in terms of multipoles. The difficulty in doing so is that the electric field is expressed in terms of *outgoing* partial waves in the coordinates of object β, while according to Eq. (3.7), the multipoles involve partial waves $\mathbf{\Psi}^{\rm reg}_{lm}(\mathbf{x}_\alpha)$ that are *regular* at the origin $\mathcal{O}_\alpha$, in the coordinates of object α. Going from the outgoing to the regular vector solutions and changing the coordinate system involves a translation and change of basis which can be expressed as $\mathbf{\Psi}^{\rm out}_{lm}(\mathbf{x}_\alpha \pm d\hat{\mathbf{z}}) = \sum_{l'm'} U^{\pm}_{l'm'lm}\mathbf{\Psi}^{\rm reg}_{l'm'}(\mathbf{x}_\alpha)$ where the *universal* (shape and material independent) translation matrices $\mathbb{U}^{21}$ and $\mathbb{U}^{12}$ represent the interaction between the multipoles. For fixed (lm), $(l'm')$, they are 2×2 matrices (magnetic and electric multipoles), and functions of kd only. Their explicit form is known but not provided here to save space [24]; they fall off with kd according to classical expectations for the EM field. Then the electric field becomes $\frac{1}{ik}\mathbf{E}_\beta(\mathbf{x}_\alpha \pm d\hat{\mathbf{z}}) = \sum_{lm}\phi^\beta_{lm}\mathbf{\Psi}^{\rm reg}_{lm}(\mathbf{x}_\alpha)$ with $\phi^\beta_{lm} = i\sum_{lm} U^{21(12)}_{lml'm'}Q^\beta_{l'm'}$, and the integration in Eq. (3.6) leads, using Eq. (3.7), to the off-diagonal terms in Eq. (3.8).

Diagonal terms — The self-action, given by the second term of Eq. (3.6), is more interesting and more challenging. It can be expressed in terms of multipoles if we use the constraint for the currents, Eqs. (3.3) and (3.4). To do so, we first note that in scattering theory one usually knows the incident solution and would like to find the outgoing scattered solution. They are related by the S-matrix. Here the situation is slightly different. We seek to relate a regular solution $\mathbf{E}_0(\mathbf{x}_\alpha) = ik\sum_{lm}\phi_{0,lm}\mathbf{\Psi}^{\rm reg}_{lm}(\mathbf{x}_\alpha)$ and the outgoing scattered solution, $\mathbf{E}_\alpha(\mathbf{x}_\alpha) = -k\sum_{lm} Q^\alpha_{lm}\mathbf{\Psi}^{\rm out}_{lm}(\mathbf{x}_\alpha)$, generated by the currents in the material — a relation determined by the T-matrix, $\mathbb{T}^\alpha \equiv (\mathbb{S}^\alpha - \mathbb{I})/2$ — schematically $i\mathbf{Q}^\alpha = \mathbb{T}^\alpha\boldsymbol{\phi}_0$ [*] [25]. We face the inverse problem of determining $\phi_{0,lm}$ for known scattering data Q^α_{lm}, hence,

$$\phi_{0,lm} = i\sum_{l'm'}[T^\alpha]^{-1}_{lml'm'}Q^\alpha_{l'm'} \tag{3.9}$$

[+] The two components of $\mathbf{\Psi}^{\rm reg}_{lm}$ are given by $1/k$ times the weights for E- and M-multipoles of Eq. (3.7) with Y^*_{lm} replaced by Y_{lm}. Similarly, $\mathbf{\Psi}^{\rm out}_{lm}$ have the same expressions upon substituting Bessel by Hankel functions, $j_l \to h^{(1)}_l$.

[*] Our relation between S- and T-matrix follows Ref. [25] and hence deviates from usual conventions by a factor i.

so that the incident field is given in terms of the S-matrix, as indicated in Eq. (3.4). Next, we express the self-action of the currents inside a body (the second term of Eq. (3.6)), as $S_k^\alpha[\mathbf{J}_\alpha] = \frac{1}{2}\int d\mathbf{x}_\alpha[\mathbf{E}\mathbf{D}^* - \mathbf{B}\mathbf{H}^* - (\mathbf{E}_0\mathbf{D}_0^* - \mathbf{B}_0\mathbf{H}_0^*)]$, the change of the field action that results from placing the body into the *fixed* (regular) incident field $\mathbf{E}_0 = \mathbf{D}_0$, $\mathbf{H}_0 = \mathbf{B}_0$, where $\mathbf{E}$, $\mathbf{H}$ and $\mathbf{D}$, $\mathbf{B}$ are the new total fields and fluxes in the presence of the body. Using $\mathbf{D} = \epsilon_\alpha \mathbf{E}$, $\mathbf{H} = \mu_\alpha^{-1}\mathbf{B}$ inside the body and Eq. (3.3), straightforward manipulations lead to the simple self-action $S_k^\alpha[\mathbf{J}_\alpha] = -\frac{1}{2ik}\int d\mathbf{x}_\alpha \mathbf{J}_\alpha^* \mathbf{E}_0(\{\mathbf{J}_\alpha, \mathbb{S}^\alpha\})$. If we substitute the regular wave expansion for $\mathbf{E}_0$ with coefficients of Eq. (3.9) and integrate by using Eq. (3.7), we get Eq. (3.8).

Having established the action for electric and magnetic multipoles, Eq. (3.7), the Casimir energy follows in complete analogy to the scalar case by integrating over the multipoles. Hence, the Casimir energy for two objects is again given by Eq. (2.40) with an additional factor of 1/2 since the electromagnetic field is real valued.

4. Applications: Scalar field

In this section we give a few typical applications of our method for a scalar field. We consider a *real* scalar field fluctuating in the space between two spheres on which Robin boundary conditions, $\phi - \lambda_\alpha \partial_n \phi = 0$, are imposed. Because a real field has half the oscillation modes of a complex field, the Casimir energy in Eq. (2.40) must be divided by 2, giving

$$\mathcal{E}_2[\mathcal{C}] = \frac{\hbar c}{2\pi}\int_0^\infty d\kappa \ln\det(1 - \mathbb{T}^1\mathbb{U}^{12}\mathbb{T}^2\mathbb{U}^{21})\,. \tag{4.1}$$

We allow for different Robin parameters $\lambda_{1,2}$ at the spheres of radius R. This choice allows us to study Dirichlet ($\lambda/R \to 0$) and Neumann ($\lambda/R \to \infty$) boundary conditions on separate spheres as special cases. We obtain the Casimir energy as a series in R/d for large separations d and numerically at all separations. A comparison of the two approaches allows us to measure the rate of convergence of our results. We find that for Robin boundary conditions the sign of the force depends on the ratios λ_α/R and on the separation d.

4.1. Interaction of two spheres with Robin boundary conditions: general considerations

The Robin boundary condition $\phi - \lambda_\alpha \partial_n \phi = 0$ allows a continuous interpolation between Dirichlet and Neumann boundary conditions. Since the radius of the sphere introduces a natural length scale, it is convenient to replace λ by a dimensionless variable, $\zeta_\alpha \equiv \lambda_\alpha/R$. For $\zeta_\alpha > 0$, the modulus of the field is suppressed if the surface is approached from the outside, while for $\zeta_\alpha < 0$ it is enhanced. Hence, for negative ζ_α bound surface states can be expected. All the information about the shape of the object and the boundary conditions at its surface is provided by the $\mathbb{T}$-matrix. For spherically symmetric objects the $\mathbb{T}$-matrix is diagonal and is completely specified by phase shifts $\delta_l(k)$ that do not depend on m,

$$\mathcal{T}_{lml'm'}(k) = \delta_{ll'}\delta_{mm'}\frac{1}{2}\left(e^{2i\delta_l(k)} - 1\right) . \tag{4.2}$$

In the discussion of the $\mathbb{T}$-matrix for an individual object we again suppress the label α. The phase shifts for Robin boundary conditions are

$$\cot\delta_l(k) = \frac{n_l(\xi) - \zeta\xi\, n_l'(\xi)}{j_l(\xi) - \zeta\xi\, j_l'(\xi)} , \tag{4.3}$$

where $\xi = kR$ and j_l (n_l) are spherical Bessel functions of first(second) kind. To apply Eq. (4.1), we have to evaluate the matrix elements of the transition matrices for imaginary frequencies $k = i\kappa$. Using $j_l(iz) = i^l\sqrt{\pi/(2z)}I_{l+1/2}(z)$ and $h_l^{(1)}(iz) = -i^{-l}\sqrt{2/(\pi z)}K_{l+1/2}(z)$, we obtain for the $\mathbb{T}$-matrix elements

$$\mathcal{T}_{lmlm}(i\kappa) = (-1)^l\frac{\pi}{2}\frac{(1/\zeta + 1/2)I_{l+1/2}(z) - zI_{l+1/2}'(z)}{(1/\zeta + 1/2)K_{l+1/2}(z) - zK_{l+1/2}'(z)} , \tag{4.4}$$

where $z \equiv \kappa R$.

For two spherical objects we can assume that the center-to-center distance vector is parallel to the z-axis. Then the translation matrices simplify. For imaginary frequencies the translation matrix elements become

$$\begin{aligned}\mathcal{U}_{l'mlm}^{\left\{\begin{smallmatrix}12\\21\end{smallmatrix}\right\}}(d) = & -(-1)^m i^{-l'+l}\sqrt{(2l+1)(2l'+1)} \\ & \times \sum_{l''}(\pm 1)^{l''}(2l''+1)\begin{pmatrix} l & l' & l'' \\ 0 & 0 & 0\end{pmatrix}\begin{pmatrix} l & l' & l'' \\ m & -m & 0\end{pmatrix} K_{l''+1/2}(\kappa d) ,\end{aligned} \tag{4.5}$$

where d is the separation distance.

An analysis of the $\mathbb{T}$-matrix shows that it has poles for $-1 < \zeta < 0$. For any ζ in this interval, there exists a finite number of bound states, which increases as $\zeta \to 0$. In the following, we restrict to $\zeta \geq 0$ and leave the study of interactions in the presence of bound states to a future publication.

The special case of spheres with Dirichlet boundary conditions has been studied in Ref. [15]. For two spheres of equal radius, the matrix $\sum_{l''} A_{ll''}^{(m)} A_{l''l'}^{(m)}$ in the notation of Ref. [15] is proportional to our $\mathbb{T}^1\mathbb{U}^{12}\mathbb{T}^2\mathbb{U}^{21}$ times $K_{l+1/2}(\kappa R)/K_{l'+1/2}(\kappa R)$. It is easy to see that this proportionality factor drops out in the final result for the energy if one uses $\ln\det = \operatorname{tr}\ln$ in Eq. (4.1) and expands the logarithm around unity. Thus we agree with the results given in Ref. [15].

4.2. Asymptotic expansion for large separation

In this section we consider the Casimir interaction between two spheres due to a scalar field obeying Robin boundary conditions, allowing for a different parameter $\lambda_{1,2}$ on each sphere. The Casimir energy can be developed in an asymptotic expansion in R/d using

$\ln\det = \operatorname{tr}\ln$ in Eq. (4.1). Expanding the logarithm in powers of $\mathbb{N} = \mathbb{T}^1\mathbb{U}^{12}\mathbb{T}^2\mathbb{U}^{21}$, since the $\mathbb{T}$-matrix has no poles in the region of interest we get

$$\mathcal{E} = -\frac{\hbar c}{2\pi}\int_0^\infty d\kappa \sum_{p=1}^{\infty}\frac{1}{p}\operatorname{tr}\left(\mathbb{N}^p\right) . \tag{4.6}$$

We have performed the matrix operations using `Mathematica`. The scaling of the $\mathbb{T}$-matrix at small κ shows that the p^{th} power of $\mathbb{N}$ (corresponding to $2p$ scatterings) becomes important at order $d^{-(2p+1)}$. Partial waves of order l start to contribute at order $d^{-(3+2l)}$ if the $\mathbb{T}$-matrix is diagonal in l, which is the case for spherically symmetric objects. Hence the leading terms with $p = 1$ and $l = 0$ yield the exact energy to order d^{-4}. In the following we will usually restrict the expansion to $p \leq 3$, $l \leq 2$, yielding the interaction to order d^{-8}.

The large distance expansion of the Casimir energy can be written as

$$\mathcal{E} = \frac{\hbar c}{\pi}\frac{1}{d}\sum_{j=3}^{\infty} b_j \left(\frac{R}{d}\right)^{j-1} , \tag{4.7}$$

where b_j is the coefficient of the term $\sim d^{-j}$. These coefficients can be computed for general Robin boundary conditions [7]. Here we restrict to the limiting cases of Dirichlet and Neumann boundary conditions. An interesting property is that some coefficients b_j go to zero for $\lambda_\alpha \to \infty$, which corresponds to Neumann boundary conditions. If both λ_α go to infinity, the coefficients b_j vanish for $j = 1, \ldots, 6$, so that the leading term in the Casimir energy is $\sim d^{-7}$ with a negative amplitude. Hence, Neumann boundary conditions lead to an attractive Casimir-Polder power law, as is known from electromagnetic field fluctuations. This result can be understood from the absence of low-frequency s-waves for Neumann boundary conditions. It is clearly reflected by the low frequency expansion of the $\mathbb{T}$-matrix, which has a vanishing amplitude for $\lambda_\alpha \to \infty$ if $l = 0$. If one $\lambda_\alpha = 0$ and the other goes to infinity, only the coefficients b_3 and b_4 vanish so that the energy scales as d^{-5} with a *positive* amplitude. In general, one has $b_3 < 0$ for $\lambda_\alpha \geq 0$, so that at asymptotic distances the Casimir force is attractive for all non-negative finite λ_α, and for λ_α both infinite. It is repulsive if one λ_α is finite and the other infinite, i.e., if one sphere obeys Neumann boundary conditions. However, at smaller distances the interaction can change sign depending on λ_α, as shown below.

More precisely, we obtain the following results. If both $\lambda_\alpha = 0$, the field obeys Dirichlet conditions at the two spheres and the first six coefficients are

$$b_3 = -\frac{1}{4}, \quad b_4 = -\frac{1}{4}, \quad b_5 = -\frac{77}{48}, \quad b_6 = -\frac{25}{16}, \quad b_7 = -\frac{29837}{2880}, \quad b_8 = -\frac{6491}{1152} . \tag{4.8}$$

If Neumann conditions are imposed on both surfaces, the coefficients are

$$b_3 = 0, \quad b_4 = 0, \quad b_5 = 0, \quad b_6 = 0, \quad b_7 = -\frac{161}{96}, \quad b_8 = 0, \quad b_9 = -\frac{3011}{192} \quad b_{10} = -\frac{175}{128} , \tag{4.9}$$

clearly showing that the asymptotic interaction has a Casimir-Polder power law $\sim \mathcal{O}(d^{-7})$. Also, as in the electromagnetic case, the next to leading order $\mathcal{O}(d^{-8})$ vanishes [6]. Therefore we have included the two next terms of the series. For mixed Dirichlet/Neumann boundary conditions, we obtain

$$b_3 = 0, \quad b_4 = 0, \quad b_5 = \frac{17}{48}, \quad b_6 = \frac{11}{32}, \quad b_7 = \frac{663}{160}, \quad b_8 = \frac{235}{144}\,. \tag{4.10}$$

It is important to note that the series in Eq. (4.7) is an asymptotic series and therefore cannot be used to obtain the interaction at short distances.

4.3. Numerical results for Robin boundary conditions on two spheres at all separations

The primary application of our analysis is to compute the Casimir energy and force to high accuracy over a broad range of distances. However, to obtain the interaction at all distances, Eq. (4.1) has to be evaluated numerically. We shall see that the domain where our method is *least* accurate is when the two surfaces approach one another. That is the regime where semiclassical methods like the proximity force approximation (PFA) become exact. Because of its role in this limit, and because it is often used (with little justification) over wide ranges of separations, it is important to compare our calculations with the PFA predictions.

In the proximity force approximation, the energy is obtained as an integral over infinitesimal parallel surface elements at their local distance L, measured perpendicular to a surface Σ that can be one of the two surfaces of the objects, or an auxiliary surface placed between the objects. The PFA approximation for the energy is then given by

$$\mathcal{E}_{\text{PFA}} = \frac{1}{A}\int_\Sigma \mathcal{E}_{\|}(L) dS\,, \tag{4.11}$$

where $\mathcal{E}_{\|}(L)/A$ is the energy per area for two parallel plates with distance L. The Casimir energy for parallel plates with Robin boundary conditions has been obtained as function of λ_α/L in Ref. [7]. The behavior of the PFA at asymptotically small or large λ_α/L determines the Casimir interaction as $L \to 0$. For all non-zero values of $\lambda_{1,2}$, we take $\lambda_\alpha/L \to \infty$, but for the Dirichlet case, $\lambda = 0$, the limit $\lambda_\alpha/L \to 0$ applies. For parallel plates with Robin boundary conditions, in the limit $\lambda_{1,2}/L \gg 1$ we obtain the result for Neumann boundary conditions on both plates,

$$\Phi(\lambda_1/L, \lambda_2/L) \to \Phi_0^- = -\frac{\pi^2}{1440}\,, \tag{4.12}$$

and for $\lambda_{1,2}/L \ll 1$ we obtain the identical result for plates with Dirichlet conditions. Finally for $\lambda_{1,2}/L \ll 1 \ll \lambda_{2,1}/L$, we obtain the parallel plate result for unlike (Dirichlet/Neumann) boundary conditions,

$$\Phi(\lambda_1/L, \lambda_2/L) \to \Phi_0^+ = -\frac{7}{8}\Phi_0^- = \frac{7\pi^2}{11520}\,. \tag{4.13}$$

The last case is relevant at short distances if one of the $\lambda_\alpha = 0$. For two spheres of radius R and center-to-center separation d with Robin boundary conditions, the PFA results can now be obtained easily from Eq. (4.11). In terms of the surface-to-surface distance $L = d - 2R$, we get

$$\mathcal{E}_{\text{PFA}} = \Phi_0^{\pm} \frac{\pi}{2} \frac{R\,\hbar c}{(d-2R)^2}\,, \tag{4.14}$$

where the + applies if one and only one $\lambda_\alpha = 0$, and the − in all other cases. Hence, at small separation the interaction becomes independent of λ_α, in the sense that it only depends on whether one λ_α is zero.

With the results obtained above, we can analyze the sign of the interaction between plates and spheres at both asymptotically large and small distances. Since the PFA result is expected to hold in the limit where the distance tends to zero, Eq. (4.14) predicts the sign of the interaction between spheres in the limit of vanishing distance. In the limit of large distances, we can compare the results for parallel planes from Eqs. (4.12) and (4.13) to our calculations for two spheres. We find that the *sign* of the asymptotic interaction depends on the choice for λ_α and is *identical* for plates and spheres. Hence, we obtain a complete characterization of the sign of the interaction at asymptotically large and small distances for the plate and sphere geometry, which is summarized in Table 1. However, as we have seen above, the power law decay at large distance is quite different for plates and spheres.

λ_1	λ_2	$L \to 0$	$L \to \infty$	remark
0	0	−	−	− for all L
∞	0	+	+	+ for all L
∞	∞	−	−	− for all L
$]0,\infty[$	$]0,\infty[$	−	−	+ at intermediate L for large enough ratio of λ_1, λ_2. (for plates: λ_1/λ_2 or $\lambda_2/\lambda_1 \gtrsim 2.8$)
$]0,\infty[$	0	+	−	
$]0,\infty[$	∞	−	+	

Table 1. The sign of the Casimir force between two plates and two spheres with Robin boundary conditions at asymptotically small and large surface-to-surface distance L. The sign in these two limits is identical for plates and spheres. Here "−" and "+" indicate attractive and repulsive forces, respectively.

4.3.1. Casimir forces for all separations To go beyond the analytic large distance expansion, we compute numerically the interaction between two spheres of the same radius R with Robin boundary conditions. Guided by the classification of the Casimir force according to its sign at small, intermediate and large separations, we discuss the six different cases listed in Table 1. Our numerical approach starts from Eq. (4.1).

Using the matrix elements of Eq. (4.4) and Eq. (4.5), we compute the determinant and the integral over imaginary frequency numerically. We truncate the matrices at a finite multipole order l so that they have dimension $(1+l)^2 \times (1+l)^2$, yielding a series of estimates $\mathcal{E}^{(l)}$ for the Casimir energy.

$\mathcal{E}^{(1)}$ gives the exact result for asymptotically large separations, while for decreasing separations an increasing number of multipoles has to be included. The exact Casimir energy at all separations is obtained by extrapolating the series $\{\mathcal{E}^{(l)}\}$ to $l \to \infty$. We observe an exponentially fast convergence as $|\mathcal{E}^{(l)} - \mathcal{E}| \sim e^{-\delta(d/R-2)l}$, where δ is a constant of order unity. Hence, as the surfaces approach each other for $d \to 2R$, the rate of convergence tends to zero. However, we find that the first $l = 20$ elements of the series are sufficient to obtain accurate results for the energy at a separation with $R/d = 0.48$, corresponding to a surface-to-surface distance of the spheres of $L = 0.083R$, i.e., approximately 4% of the sphere diameter. In principle our approach can be extended to even smaller separations by including higher order multipoles. However, at such small separations semiclassical approximations like the PFA start to become accurate and can be also used.

The results for Dirichlet and Neumann boundary conditions are shown in Fig. 1. All energies are divided by $\mathcal{E}_{\text{PFA}}$, given in Eq. (4.14), with the corresponding amplitude Φ_0^+ (repulsive at small separations) or Φ_0^- (attractive at small separations). For like boundary conditions, either Dirichlet or Neumann, the interaction is attractive at all separations, but for unlike boundary conditions it is repulsive. At large separations the numerical results show excellent agreement with the asymptotic expansion derived above. Note that the reduction of the energy compared to the PFA estimate at large distances depends strongly on the boundary conditions, showing the different power laws at asymptotically large separations. In the limit of a vanishing surface-to-surface distance ($R/d \to 1/2$), the energy approaches the PFA estimate in all cases. Generically, the PFA overestimates the energy: $\mathcal{E}_{\text{PFA}}$ is approached from below for $R/d \to 1/2$, except in the case of Dirichlet boundary conditions on both spheres, where the PFA underestimates the actual energy in a range of $0.3 \lesssim R/d < 1/2$. The deviations from the PFA are most pronounced for Neumann boundary conditions. At a surface-to-surface distance of $L = 3R$ ($R/d = 0.2$), the PFA overestimates the energy by a factor of 100.

Casimir interactions for Robin boundary conditions with finite λ_α are shown in Fig. 2. If $\lambda_1 = \lambda_2$ the interaction is always attractive. If the λ_α are not equal and their ratio is sufficiently large, the Casimir force changes sign either once or twice. This behavior resembles the interaction of two plates with Robin boundary conditions. However, the criterion for the existence of sign changes in the force now depends not only on λ_1/λ_2, but on both quantities λ_1/R and λ_2/R separately. Even with λ_1/λ_2 fixed, for smaller λ_α/R there can be sign changes in the force, while for larger λ_α/R the force is attractive at all distances. When the ratio λ_1/λ_2 is sufficiently large (or formally infinite for Dirichlet or Neumann boundary conditions), we can identify three different generic cases where sign changes in the force occur:

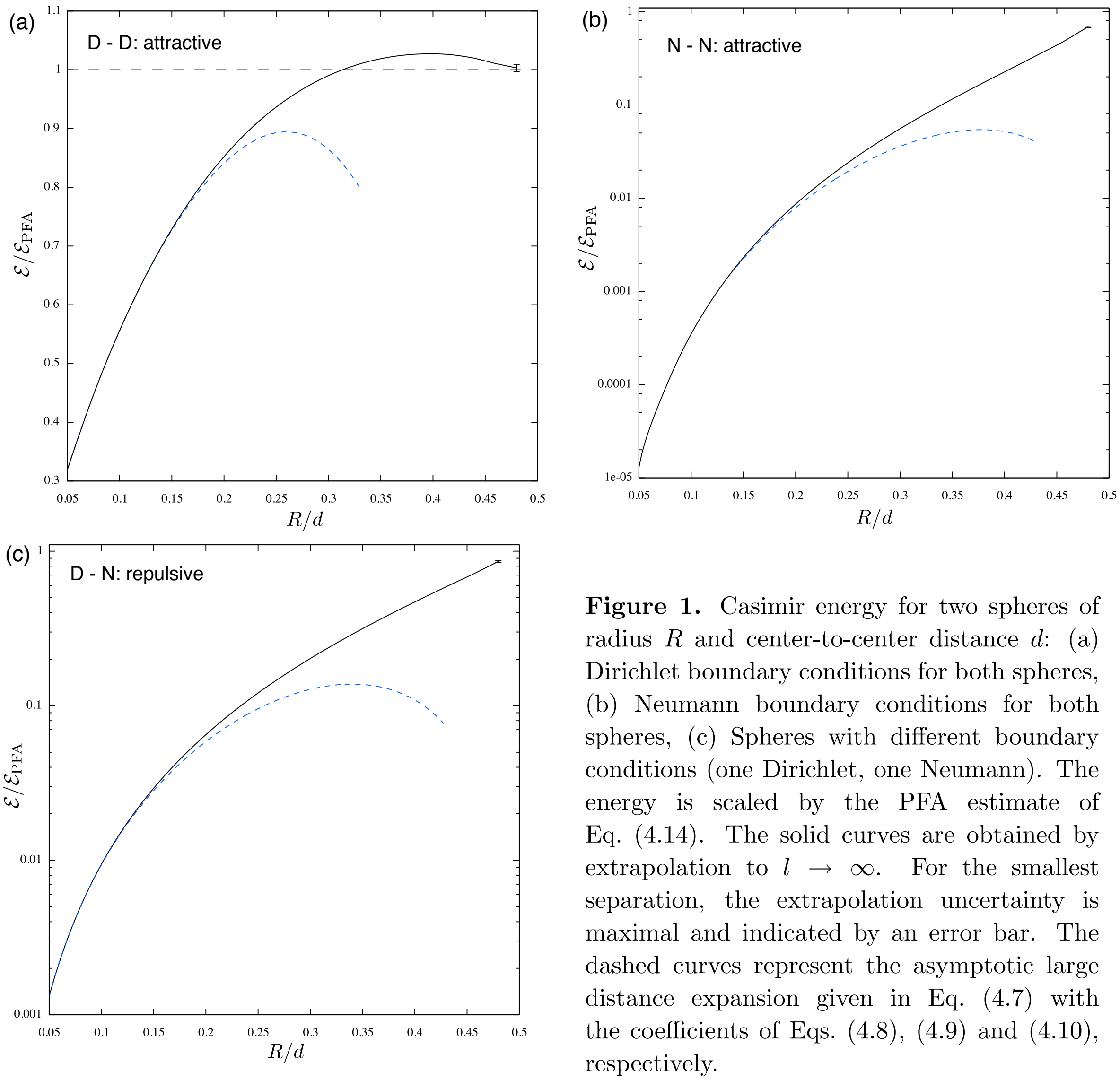

Figure 1. Casimir energy for two spheres of radius R and center-to-center distance d: (a) Dirichlet boundary conditions for both spheres, (b) Neumann boundary conditions for both spheres, (c) Spheres with different boundary conditions (one Dirichlet, one Neumann). The energy is scaled by the PFA estimate of Eq. (4.14). The solid curves are obtained by extrapolation to $l \to \infty$. For the smallest separation, the extrapolation uncertainty is maximal and indicated by an error bar. The dashed curves represent the asymptotic large distance expansion given in Eq. (4.7) with the coefficients of Eqs. (4.8), (4.9) and (4.10), respectively.

- First, we consider Dirichlet boundary conditions ($\lambda_1 = 0$) on one sphere and a finite non-vanishing λ_2/R at the other sphere. Figure 2(a) displays the energy for $\lambda_2/R = 10$ as a typical example. At large distances the energy is negative, while it is positive at short separations with one sign change in between. The asymptotic expansion of Eq. (4.7) yields the exact energy at separations well below the sign change [7]. While the expansion predicts qualitatively the correct overall behavior of the energy, it does not yield the actual position of the sign change correctly. Of course, for the Casimir interaction between compact objects, the sign of the force $\mathcal{F} = -\partial\mathcal{E}/\partial d$ is the physically important quantity, not the energy. The distance at which the force vanishes cannot be deduced directly from the slope of the curve for $\hat{\mathcal{E}} \equiv \mathcal{E}/\mathcal{E}_{\rm PFA}$, since one has

$$\hat{\mathcal{E}}'(d) = \frac{1}{\mathcal{E}_{\rm PFA}(d)}\left[\mathcal{E}'(d) + \frac{2}{d-2R}\mathcal{E}(d)\right]. \qquad (4.15)$$

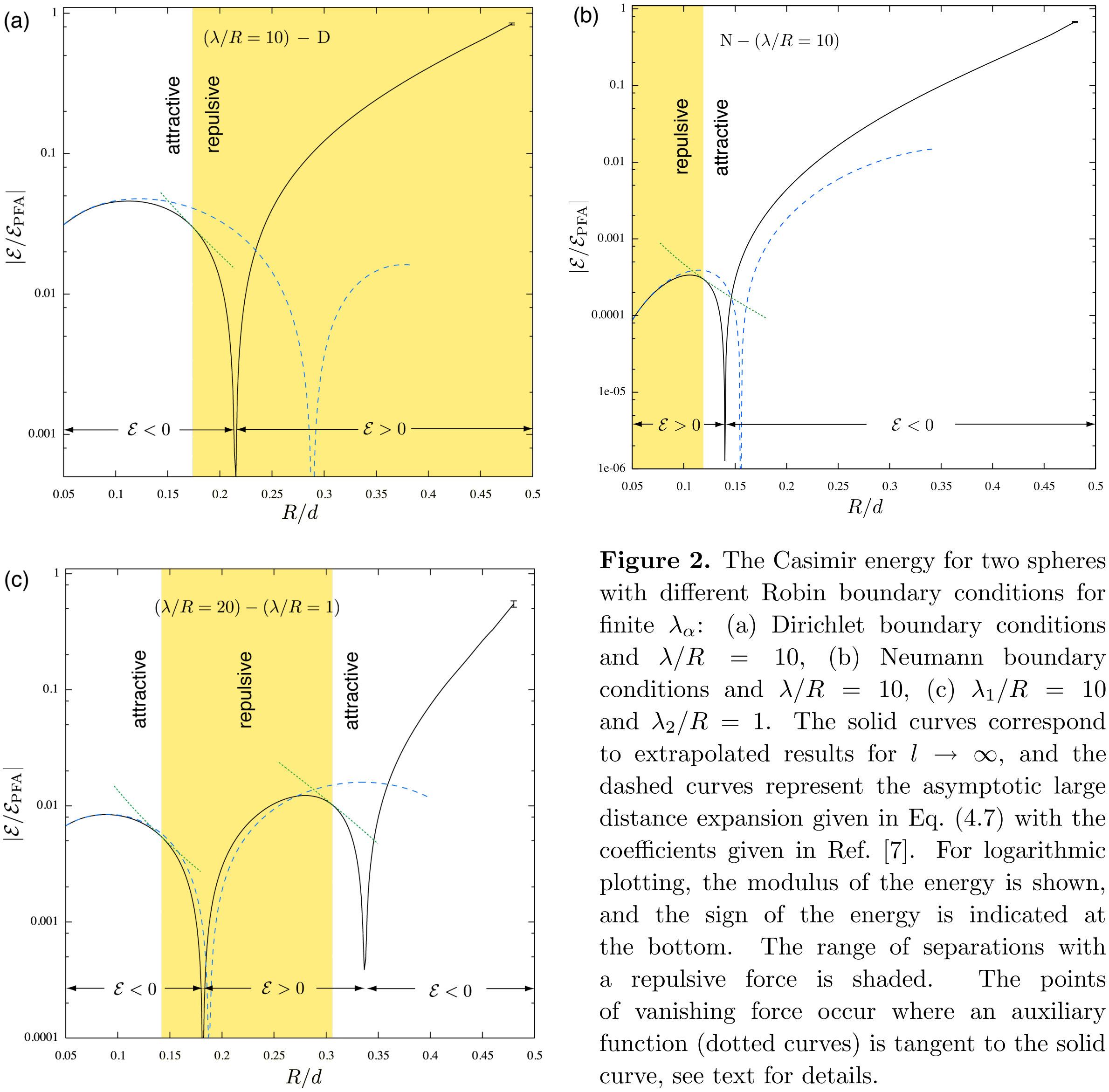

Figure 2. The Casimir energy for two spheres with different Robin boundary conditions for finite λ_α: (a) Dirichlet boundary conditions and $\lambda/R = 10$, (b) Neumann boundary conditions and $\lambda/R = 10$, (c) $\lambda_1/R = 10$ and $\lambda_2/R = 1$. The solid curves correspond to extrapolated results for $l \to \infty$, and the dashed curves represent the asymptotic large distance expansion given in Eq. (4.7) with the coefficients given in Ref. [7]. For logarithmic plotting, the modulus of the energy is shown, and the sign of the energy is indicated at the bottom. The range of separations with a repulsive force is shaded. The points of vanishing force occur where an auxiliary function (dotted curves) is tangent to the solid curve, see text for details.

The force vanishes at the distance d_0 if $\mathcal{E}'(d_0) = 0$, so that

$$\hat{\mathcal{E}}'(d_0) = \frac{2}{d_0 - 2R}\hat{\mathcal{E}}(d_0)\,. \tag{4.16}$$

Hence the distance at which the force vanishes is determined by the position d_0 where the curve of the auxiliary function $t(d) = \tau(d/R-2)^2$ is tangent to the curve of $\hat{\mathcal{E}}$. The two unknown quantities d_0 and τ are then determined by the conditions $\hat{\mathcal{E}}(d_0) = t(d_0)$ and $\hat{\mathcal{E}}'(d_0) = t'(d_0)$. This procedure allows us to obtain the distance at which the force vanishes easily, without computing derivatives numerically. The tangent segment of the curve for $t(d)$ is shown in Fig. 2(a) as a dotted line. From this construction we find that at a distance $d_{-\Rightarrow+}$ the force changes from attractive to repulsive for decreasing separations. The position $d_{-\Rightarrow+}$ corresponds to a minimum of the energy and decreases with decreasing λ_2/R, so that in the limit $\lambda_2/R \to 0$ it approaches the case of two spheres with Dirichlet boundary conditions, where the force is always attractive.

- Second, we study Neumann boundary conditions on one sphere and a finite non-vanishing λ_2/R at the other sphere. As an example we choose again $\lambda_2/R = 10$, as shown in Fig. 2(b). The energy is positive at large distances and becomes negative at small distances. The asymptotic expansion is found to be valid well below the separation where the sign of the energy changes [7]. Hence, the expansion describes the behavior of the energy qualitatively, but does not predict the precise position of the sign change. The sign change of the force can be obtained by the method described above. At a position $d_{+\Rightarrow-}$, the force changes from repulsive to attractive with decreasing separation and the energy is maximal. A decreasing (increasing) λ_2/R shifts $d_{+\Rightarrow-}$ to smaller (larger) separations. This result is consistent with an entirely repulsive (attractive) force for Neumann-Dirichlet (Neumann-Neumann) boundary conditions.
- The third case is obtained if both λ_α are finite and non-zero. A typical example with $\lambda_1/R = 20$ and $\lambda_2/R = 1$ is shown in Fig. 2(c). The energy is negative both at large and small separations but turns positive at intermediate distances. The asymptotic expansion applies again at sufficiently large separations beyond the position where the energy becomes positive. For values of the ratio λ_1/λ_2 that are larger than an R-dependent threshold, the force changes sign twice, so that it is repulsive between the separations $d_{-\Rightarrow+}$ and $d_{+\Rightarrow-}$. The energy has a minimum (maximum) at $d_{-\Rightarrow+}$ ($d_{+\Rightarrow-}$). If λ_1/R increases and λ_2/R decreases, the repulsive region grows until eventually the force becomes repulsive at all separations, corresponding to the limit of Dirichlet/Neumann boundary conditions. Decreasing λ_1/R and increasing λ_2/R reduces the interval with repulsion. In this case, first the zeros of the energy disappear, leaving negative energy at all distances but still a repulsive region, and then the two positions where the force vanishes merge, leaving an entirely attractive force.

5. Applications: Electromagnetic field

As a specific example for the electromagnetic field, we consider two identical dielectric spheres. Due to symmetry, the multipoles are decoupled so that the T-matrix is diagonal,

$$T^{11}_{lmlm} = (-1)^l \frac{\pi}{2} \frac{\eta I_{l+\frac{1}{2}}(z)\left[I_{l+\frac{1}{2}}(nz) + 2nzI'_{l+\frac{1}{2}}(nz)\right] - nI_{l+\frac{1}{2}}(nz)\left[I_{l+\frac{1}{2}}(z) + 2zI'_{l+\frac{1}{2}}(z)\right]}{\eta K_{l+\frac{1}{2}}(z)\left[I_{l+\frac{1}{2}}(nz) + 2nzI'_{l+\frac{1}{2}}(nz)\right] - nI_{l+\frac{1}{2}}(nz)\left[K_{l+\frac{1}{2}}(z) + 2zK'_{l+\frac{1}{2}}(z)\right]}, \tag{5.1}$$

where the sphere radius is R, $z = \kappa R$, $n = \sqrt{\epsilon(i\kappa)\mu(i\kappa)}$, $\eta = \sqrt{\epsilon(i\kappa)/\mu(i\kappa)}$, and $I_{l+\frac{1}{2}}$, $K_{l+\frac{1}{2}}$ are Bessel functions. T^{22}_{lmlm} is obtained from Eq. (5.1) by interchanging ϵ and μ. For all partial waves, the *leading* low frequency contribution is determined by the *static* electric multipole polarizability, $\alpha_l^{\mathrm{E}} = [(\epsilon-1)/(\epsilon+(l+1)/l)]R^{2l+1}$, and the corresponding magnetic polarizability, $\alpha_l^{\mathrm{M}} = [(\mu-1)/(\mu+(l+1)/l)]R^{2l+1}$. Including the next to leading terms, the T-matrix has the structure

$$T^{11}_{lmlm} = \kappa^{2l}\left[\frac{(-1)^{l-1}(l+1)\alpha_l^{\mathrm{M}}}{l(2l+1)!!(2l-1)!!}\kappa + \gamma_{l3}^{\mathrm{M}}\kappa^3 + \gamma_{l4}^{\mathrm{M}}\kappa^4 + \ldots\right],$$

and T^{22}_{lmlm} is obtained by $\alpha_l^{\mathrm{M}} \to \alpha_l^{\mathrm{E}}$, $\gamma_{ln}^{\mathrm{M}} \to \gamma_{ln}^{\mathrm{E}}$. The first terms are $\gamma_{13}^{\mathrm{M}} = -[4+\mu(\epsilon\mu+\mu-6)]/[5(\mu+2)^2]R^5$, $\gamma_{14}^{\mathrm{M}} = (4/9)[(\mu-1)/(\mu+2)]^2R^6$, and γ_{13}^{E}, γ_{14}^{E} are obtained again by the replacement, $\mu \to \epsilon$. Now we can apply our general formula in Eq. (2.40) (with a factor of 1/2 and the translation matrices for the electromagnetic field [24]) to two dielectric spheres with center-to-center distance d. For simplicity, we restrict to two partial waves ($l = 2$) and two scatterings ($p = 1$), which yields the exact Casimir energy to order d^{-10}. Matrix operations are performed with `Mathematica`, and we find the interaction

$$\begin{aligned}\mathcal{E} = -\frac{\hbar c}{\pi}\Bigg\{&\left[\frac{23}{4}\left((\alpha_1^{\mathrm{E}})^2 + (\alpha_1^{\mathrm{M}})^2\right) - \frac{7}{2}\alpha_1^{\mathrm{E}}\alpha_1^{\mathrm{M}}\right]\frac{1}{d^7}\\
&+ \frac{9}{16}\left[\alpha_1^{\mathrm{E}}\left(59\alpha_2^{\mathrm{E}} - 11\alpha_2^{\mathrm{M}} + 86\gamma_{13}^{\mathrm{E}} - 54\gamma_{13}^{\mathrm{M}}\right) + \mathrm{E}\leftrightarrow\mathrm{M}\right]\frac{1}{d^9}\\
&+ \frac{315}{16}\left[\alpha_1^{\mathrm{E}}\left(7\gamma_{14}^{\mathrm{E}} - 5\gamma_{14}^{\mathrm{M}}\right) + \mathrm{E}\leftrightarrow\mathrm{M}\right]\frac{1}{d^{10}} + \ldots\Bigg\},\end{aligned} \tag{5.2}$$

where E ↔ M indicates terms with exchanged superscripts. The leading term, $\sim d^{-7}$, has precisely the form of the Casimir-Polder force between two atoms [8], including magnetic effects [9]. The higher order terms are new, and provide the first systematic result for dielectrics with strong curvature. There is no $\sim 1/d^8$ term.

The limit of perfect metals follows for $\epsilon \to \infty$, $\mu \to 0$. Then higher orders are easily included, yielding an asymptotic series

$$\mathcal{E} = -\frac{\hbar c}{\pi}\frac{R^6}{d^7}\sum_{n=0}^{\infty} c_n \left(\frac{R}{d}\right)^n, \tag{5.3}$$

where the first 10 coefficients are $c_0 = 143/16$, $c_1 = 0$, $c_2 = 7947/160$, $c_3 = 2065/32$, $c_4 = 27705347/100800$, $c_5 = -55251/64$, $c_6 = 1373212550401/144506880$, $c_7 = -7583389/320$, $c_8 = -2516749144274023/44508119040$, $c_9 = 274953589659739/275251200$. This series is obtained by expanding in powers of $\mathbb{N}$ and frequency κ, and does not converge for any fixed R/d. To obtain the energy at all separations, one has to compute Eq. (2.40) without these expansions. This is done as before in the case of a scalar field: We truncate the matrix $\mathbb{N}$ at a finite multipole order l, and compute the determinant and the integral numerically. The result is shown in Fig. 3 for perfect metal spheres. Our data indicate again that the energy converges as $e^{-\delta(d/R-2)l}$ to its exact value at $l \to \infty$, with $\delta \sim \mathcal{O}(1)$. Our result spans all separations between the Casimir-Polder limit for $d \gg R$, and the proximity force approximation (PFA) for $R/d \to 1/2$. At a surface-to-surface distance $L = 4R/3$ ($R/d = 0.3$), PFA overestimates the energy by a factor of 10. Including up to $l = 32$ and extrapolating based on the exponential fit, we

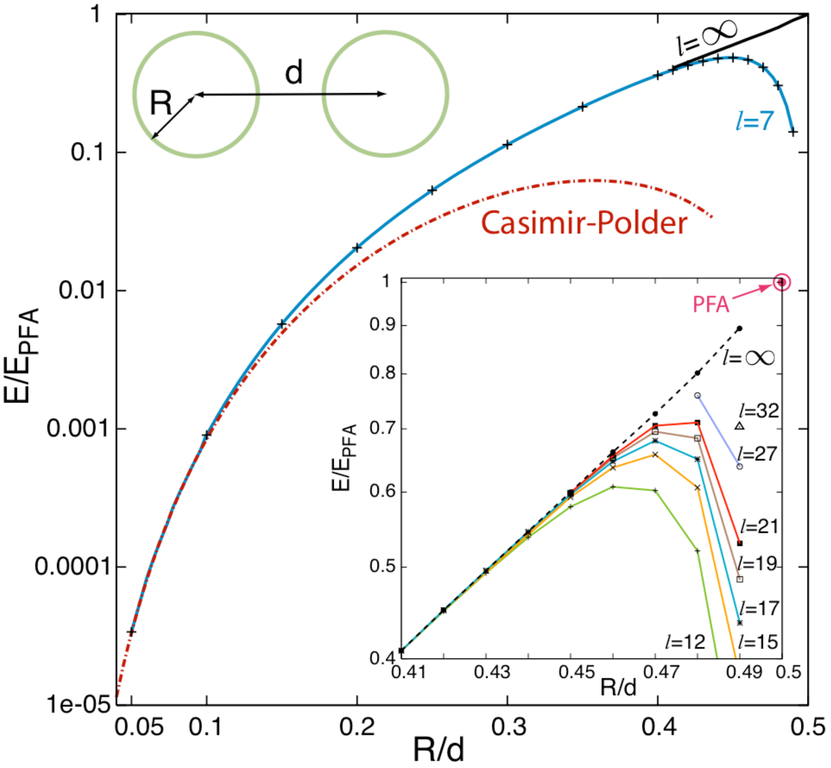

Figure 3. Casimir energy of two metal spheres, divided by the PFA estimate $\mathcal{E}_{\rm PFA} = -(\pi^3/1440)\hbar c R/(d-2R)^2$, which holds only in the limit $R/d \to 1/2$. The label l denotes the multipole order of truncation. The curves $l = \infty$ are obtained by extrapolation. The Casimir-Polder curve is the leading term of Eq. (5.3). Inset: Convergence at short separations.

can accurately determine the Casimir energy down to $R/d = 0.49$, *i.e.* $L = 0.04R$. A similar numerical evaluation can be also applied to dielectrics [7].

Acknowledgments

This work was supported by the U. S. Department of Energy (DOE) under cooperative research agreement #DF-FC02-94ER40818 (RLJ), and by a Heisenberg Fellowship from the German Research Foundation (TE).

References

[1] H. B. G. Casimir, Indag. Math. **10**, 261 (1948) [Kon. Ned. Akad. Wetensch. Proc. **51**, 793 (1948)].
[2] N. Graham, R. L. Jaffe, V. Khemani, M. Quandt, O.Schroeder and H. Weigel, Nucl. Phys. B **B677**, 379 (2004) [arXiv:hep-th/0309130]; N. Graham, R. L. Jaffe, V. Khemani, M. Quandt, M. Scandurra and H. Weigel, Nucl. Phys. **B645**, 49 (2002) [arXiv:hep-th/0207120].
[3] See, for example, M. Bordag, U. Mohideen and V. M. Mostepanenko, Phys. Rept. **353**, 1 (2001) [arXiv:quant-ph/0106045].

[4] H. B. Chan, V. A. Aksyuk, R. N. Kleiman, D. J. Bishop, F. Capasso, Phys. Rev. Lett. **87**, 211801 (2001) [arXiv:quant-ph/0109046].

[5] F. Capasso, J. N. Munday, D. Iannuzzi and H. B. Chan, IEEE J. Quant. Electron. **13**, 400 (2007).

[6] T. Emig, N. Graham, R. L. Jaffe and M. Kardar, Phys. Rev. Lett., in press (2007). [arXiv:0707.1862].

[7] T. Emig, N. Graham, R. L. Jaffe, and M. Kardar, Preprint [arXiv:0710.3084].

[8] H. B. G. Casimir and D. Polder, Phys. Rev. **73**, 360 (1948).

[9] G. Feinberg and J. Sucher, Phys. Rev. A **2**, 2395 (1970).

[10] R. Balian and B. Duplantier, Ann. Phys. (New York) **104**, 300 (1977); **112**, 165 (1978).

[11] O. Kenneth and I. Klich, Phys. Rev. Lett. **97**, 160401 (2006).

[12] H. Gies, K. Langfeld and L. Moyaerts, JHEP **0306**, 018 (2003) [arXiv:hep-th/0303264].

[13] H. Gies and K. Klingmüller, Phys. Rev. D **74**, 045002 (2006) [arXiv:quant-ph/0605141].

[14] H. Gies and K. Klingmüller, Phys. Rev. Lett. **97**, 220405 (2006) [arXiv:quant-ph/0606235]

[15] A. Bulgac, P. Magierski and A. Wirzba, Phys. Rev. D **73**, 025007 (2006) [arXiv:hep-th/0511056].

[16] T. Emig, R. L. Jaffe, M. Kardar, and A. Scardicchio, Phys. Rev. Lett. **96**, 080403 (2006) [arXiv:cond-mat/0601055].

[17] H. Li and M. Kardar, Phys. Rev. Lett. **67**, 3275 (1991); Phys. Rev. A **46**, 6490 (1992).

[18] T. Emig, A. Hanke, R. Golestanian, and M. Kardar, Phys. Rev. Lett. **87**, 260402 (2001) [arXiv:cond-mat/0106028].

[19] R. Büscher and T. Emig, Phys. Rev. Lett. **94**, 133901 (2005).

[20] R. P. Feynman and A. R. Hibbs, *Quantum Mechanics and Path Integrals* (McGraw-Hill, New York, 1965).

[21] M. Bordag, D. Robaschik, and E. Wieczorek, Ann. Phys. **165**, 192 (1985).

[22] R. L. Jaffe, Phys. Rev. D **72**, 021301 (2005) [arXiv:hep-th/0503158].

[23] R. C. Wittmann, IEEE Transactions on Antennas and Propagation, **36**, 1078 (1988).

[24] See, for example, Eqs. (47), (62), (65), (66) in Ref. [23].

[25] P. C. Waterman, Phys. Rev. D **3**, 825 (1971).